









Soil texture and environmental conditions influence the biogeochemical responses of soils to drought and flooding

Kaizad F. Patel ¹, Sarah J. Fansler ¹, Tayte P. Campbell ¹, Ben Bond-Lamberty ², A. Peyton Smith ³, Taniya RoyChowdhury⁴, Lee Ann McCue ⁵, Tamas Varga ⁵ & Vanessa L. Bailey ¹✉

Climate change is intensifying the global water cycle, with increased frequency of drought and flood. Water is an important driver of soil carbon dynamics, and it is crucial to understand how moisture disturbances will affect carbon availability and fluxes in soils. Here we investigate the role of water in substrate-microbe connectivity and soil carbon cycling under extreme moisture conditions. We collected soils from Alaska, Florida, and Washington USA, and incubated them under Drought and Flood conditions. Drought had a stronger effect on soil respiration, pore-water carbon, and microbial community composition than flooding. Soil response was not consistent across sites, and was influenced by site-level pedological and environmental factors. Soil texture and porosity can influence microbial access to substrates through the pore network, driving the chemical response. Further, the microbial communities are adapted to the historic stress conditions at their sites and therefore show site-specific responses to drought and flood.

¹Pacific Northwest National Laboratory, Biological Sciences Division, Richland, WA, USA. ²Pacific Northwest National Laboratory, Joint Global Change Research Institute, College Park, MD, USA. ³Texas A&M University, Agrilife, Soil and Crop Sciences Dept., College Station, TX, USA. ⁴USDA Agricultural Research Service, Crops Pathology and Genetics Research Unit, Davis, CA, USA. ⁵Pacific Northwest National Laboratory, Environmental and Molecular Sciences Division, Richland, WA, USA. ✉email: vanessa.bailey@pnnl.gov

The timing and distribution of precipitation are projected to change under climate change, increasing the frequency of drought in some locations and extreme inundation events, including storms and storm surges, in others^{1,2}. Such extreme moisture conditions drive key soil processes in ways we cannot currently predict^{3,4}. For example, antecedent moisture conditions have been shown to exert an overwhelming effect on the moisture response of soil carbon dioxide (CO₂) fluxes^{5–7}, including the increased CO₂ fluxes that occur during rewetting^{8–10}. The mechanisms behind this amplified respiration response, often described as the “Birch effect”, remain ill-defined, as this is a complex phenomenon arising from various physicochemical and biochemical destabilization processes that collectively increase microbial oxidation of soil organic carbon (SOC)^{9,11–13}. With the continued intensification of the global water cycle^{14,15}, it is imperative to understand how a complex soil biogeochemical system functions under moisture extremes, such as drought and flood, which could pose water stress to certain ecosystem types.

The ionic strength of soil solution varies with moisture content and can be up to nine orders of magnitude greater in dry soils compared to saturated soils¹⁶. Thus, varying moisture conditions can lead to extremely different chemical environments at the pore scale, causing selective desorption of different carbon (C) molecules from minerals; or otherwise solubilize from conditionally protected physical locations¹². Changes in soil moisture also affect soil microbial activity. Drought conditions subject soil microbes to osmotic stress in dry pores¹⁷; microbes in saturated soils have better access to SOC and nutrients, because of diffusion through the well-connected soil pore network^{18,19}. This free exchange is decreased in field-moist soils, in which the hydrologic connectivity is decreased, and some pores remain disconnected²⁰.

The objective of this work was to seek a generalized understanding of the impacts of soil water extremes (flood and drought) on soil C cycling across diverse soils, which could be attributed to microbial, chemical, or physical soil traits. We tested two hypotheses: (i) soils subjected to a simulated drought will have greater proportions of complex aromatic C species and will have greater expression of osmoprotectants; (ii) soils subjected to extended saturation will have a greater expression of motility factors (e.g., flagella and gliding motility factors).

We sampled soil cores at three locations from different climatic regions, with different drought/flooding regimes, and with soils of varying physicochemical properties: a silty soil from Caribou-Poker Creeks Research Watershed (CPCRW; Alaska, USA); a clay loam soil from a tidal freshwater near the mouth of the Columbia River (Washington State, USA), subject to frequent inundation; and a sandy soil from the headwaters of the Everglades at the Disney Wilderness Preserve (DWP; Florida, USA), subject to drying and wetting fluctuations. Cores were shipped on ice to the laboratory in Richland, WA, and each soil core was subjected to one of three randomly assigned treatments (Table 1). One set of control cores was maintained at the field-moist water content for 30 days (“field

moist”). A second set of cores was immediately saturated and incubated for 30 days (“flood”). A third set of cores was allowed to air-dry until constant weight (“drought”), and then the cores were incubated for 30 days. All treatments were conducted at 21 °C in the dark. We had two additional sets of cores as controls—“baseline” field-moist cores that were immediately deconstructed, and “time-zero saturation” cores that were saturated and immediately deconstructed for analysis.

Results and discussion

Pore-water DOC responded strongly to drought and sampling effect. To examine the influence of drying on C distribution and quality, we analyzed the dissolved organic carbon (DOC) in pore waters retained by fine (6–20 μm) and coarse (>200 μm) pore throats²¹. We expected pore-water DOC to increase in the drought-incubated soils, since drought-induced increases in ionic strength are known to destabilize adsorbed C from mineral surfaces^{12,22}. This effect was seen only for the Alaska soil, (drought: ~150 mg L⁻¹ vs. time zero: ~28 mg L⁻¹, Table 2; Dunnett’s test, $P < 0.05$ for both pore size classes). The pore-water DOC concentrations for the Florida soils appeared to decline numerically in all incubations, but these values were highly variable throughout, and there was no statistically significant pattern (Dunnett’s test, $P > 0.10$ for both pore size classes; Table 2). The Washington soils showed increased pore-water DOC across all three treatments (Table 2), suggesting a strong sampling effect, i.e., merely sampling and incubating these soils contributed to C destabilization. For these soils, DOC did not differ significantly among the three incubation treatments (ANOVA, $F = 2.58$, $P = 0.10$), and therefore these soils may be more susceptible to disturbance of handling and laboratory incubation than to the individual moisture treatments, in terms of pore-water DOC concentrations. Molecular diversity of DOC declined significantly during incubation for all soils except drought-incubated Alaska soils (Table 2).

All our cores were incubated in the laboratory, without litter inputs or amendments. As the incubations progressed, the microbial community would preferentially consume the more labile/biodegradable organic molecules, leaving behind a more uniform, protected SOM pool. This suggests that fresh C inputs, from litter or other sources, are needed to maintain SOM diversity²³. Drying and rewetting have been known to destabilize protected molecules^{12,24}, or even release osmolytes¹⁶ or microbial necromass²⁵, and it is likely that this newly available material increased SOM diversity in the silty Alaska soils.

Molecular DOC response varied by site/soil type. We characterized the DOC in the pore-water samples using ultrahigh-resolution Fourier transform ion cyclotron resonance mass spectrometry (FT-ICR-MS). Van Krevelen compound classification of FT-ICR-MS-resolved peaks is based on molecular H/C and O/C ratios^{26,27} (Supplementary Fig. S1a), and it shows that the pore-water DOC for the three sites had very different initial compositions (MANOVA, $F = 14.71$, $P < 0.001$). The Alaska soils were dominated by complex lignin-like molecules, the Florida soils by simple amino sugars and carbohydrates, and the Washington soils by protein- and lipid-like molecules (time-zero saturation in Fig. 1, and Supplementary Figs. S2 and S3).

The three soils also varied in their response to moisture changes. The Alaska soils responded most strongly to the drought treatment. Post-drought, new peaks were detected in the high-oxygen aliphatic carbohydrate- and amino sugar-like region (Fig. 2 and Supplementary Fig. S4), which was previously unique to the native, unmanipulated Florida soils (Supplementary Fig. S2). With a higher nominal oxidation state (NOSC, see Supplementary Fig. S1b), these

Table 1 Gravimetric moisture (% w/w) at which the cores were incubated.

	Field moist	Drought	Flood
Alaska	37%	<0.01% ^a	114%
Florida	9%	<0.01% ^a	36%
Washington	194%	62%	197%

Field moisture represents the soil water content when the cores were collected. Drought represents moisture content after cores were air-dried to constant weight. Flood represents moisture content after cores were saturated, using a porous ceramic plate. See “Methods” for more details.

^aThe moisture content in Alaska and Florida drought soils was below detectable levels.

Table 2 Dissolved organic carbon (DOC) concentration and molecular diversity for pore water, from coarse (>200 μm) and fine (6–20 μm) pore throats.

	Pores > 200 μm (1.5 kPa)			Pores 6–20 μm (50 kPa)		
	Alaska	Florida	Washington	Alaska	Florida	Washington
DOC concentration, $\text{mg L}^{-1}\text{C}$						
Drought	111.8 \pm 41.45*	69.02 \pm 13	13.9 \pm 2.43	186.9 \pm 62.65*	69.97 \pm 13.39	19.3 \pm 8.32
Field moist	21.22 \pm 3.73	46.33 \pm 11.94	18.68 \pm 2.36*	41.17 \pm 12.67	52.43 \pm 14.74	19.82 \pm 2.93
Flood	52.82 \pm 13.98	42.08 \pm 7.34	23.16 \pm 3.29*	63.4 \pm 20.84	82.7 \pm 16.52	24.07 \pm 2.43*
Time-zero saturation	26.3 \pm 2.78	76.68 \pm 21.76	6.03 \pm 0.57	29.14 \pm 4.41	92.33 \pm 22.22	7.28 \pm 0.34
Diversity of molecules (Shannon diversity index)						
Drought	1.53 \pm 0.01*	1.27 \pm 0.02*	1.17 \pm 0.07*	1.53 \pm 0.02*	1.33 \pm 0.01*	0.94 \pm 0.10
Field moist	1.26 \pm 0.02	1.21 \pm 0.03*	1.28 \pm 0.02*	1.01 \pm 0.00*	1.13 \pm 0.00*	1.15 \pm 0.02
Flood	1.29 \pm 0.01	1.16 \pm 0.04*	1.15 \pm 0.03	1.28 \pm 0.03*	1.28 \pm 0.04*	1.27 \pm 0.01
Time-zero saturation	1.31 \pm 0.04	1.60 \pm 0.06	1.34 \pm 0.01	1.15 \pm 0.03	1.64 \pm 0.02	1.15 \pm 0.07

Data are reported as mean \pm standard error. Asterisks denote significant differences for a given treatment compared to the time-zero control ($\alpha = 0.05$).

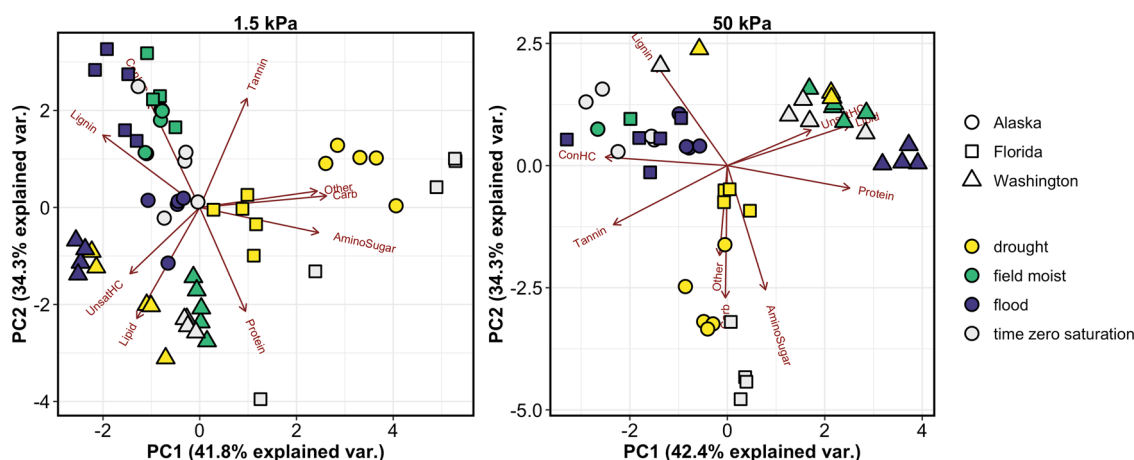


Fig. 1 Principal components analysis of Fourier transform ion cyclotron resonance mass spectrometry (FT-ICR-MS) resolved compound classes for pore-water DOC. The two panels represent coarse (>200 μm , 1.5 kPa) and fine (6–20 μm , 50 kPa) pore throats. Point shapes represent sites (circle = Alaska, square = Florida, and triangle = Washington) and colors represent treatments (yellow = drought, green = field moist, dark blue = flood, and gray = time-zero saturation). Site, treatment, and pore size all had a significant effect on DOC composition (MANOVA, $P < 0.001$).

compounds are typically more energetically favorable for microbial consumption and metabolism^{28,29}.

In contrast to this, in the Florida soils, simple aliphatic peaks were lost post-incubation and new peaks were detected in the low-O polyphenolic and aliphatic regions (Fig. 2, and Supplementary Tables S2 and S3), which represent complex molecules less favorable for microbial metabolism. This was seen across all three incubation treatments, indicating some consistency in the pore-scale chemical response to incubations under very different moisture conditions. This might suggest a stronger role of the sampling/incubation effect than the individual moisture treatments.

The Washington soils clustered tightly across all treatments, with no strong treatment effects (Fig. 1), suggesting that despite increases in pore-water DOC concentrations, there were no significant qualitative changes in the DOC composition.

Microbial gene expression responded strongly to drought. We analyzed the soils for impacts on the metagenomes and expressed genes (metatranscriptomes) directly linked to hydrologic shifts, i.e., motility and stress due to drought. The soil metagenomes for all treatments separated by site (PERMANOVA, $F = 18.22$, $P = 0.001$), but not by treatment (PERMANOVA, $F = 0.95$, $P = 0.444$;

Supplementary Fig. S5). The metagenome represents only the functional potential and not the activity of the microbial community³⁰, and our results suggest that the 30-day treatments did not alter the underlying soil functional potential for each sample site. The metatranscriptomes, on the other hand, represent microbial gene expression, which is more responsive to changes in the environment. Metatranscriptomes separated by site (PERMANOVA, $F = 5.20$, $P = 0.007$) and by treatment (PERMANOVA, $F = 3.97$, $P = 0.006$), although their interaction was not significant (PERMANOVA, $F = 1.41$, $P = 0.238$ (Supplementary Fig. S5)). The difference in the metagenome and metatranscriptome response to treatment suggests that although functional potential remained generally unchanged, the drought and flood treatments may have stimulated the activity of different genes or groups of microbes that were previously less active.

Looking at gene expression (metatranscriptomes) that differed significantly across sites (highest LDA scores, see “Methods”), there was a greater representation of anaerobic processes (reductases and nitrate respiration, Supplementary Figs. S6 and S7) in the Washington soils, whereas genes for osmoprotectant synthesis and stress responses (trehalose and ppGpp synthetases)^{31–33} were seen in the Florida soils (Supplementary Fig. S7). These results are consistent with the antecedent moisture history of these sites: the Washington soils experience regular inundation in the river floodplain and are often at/near saturation in the field, whereas the Florida soils

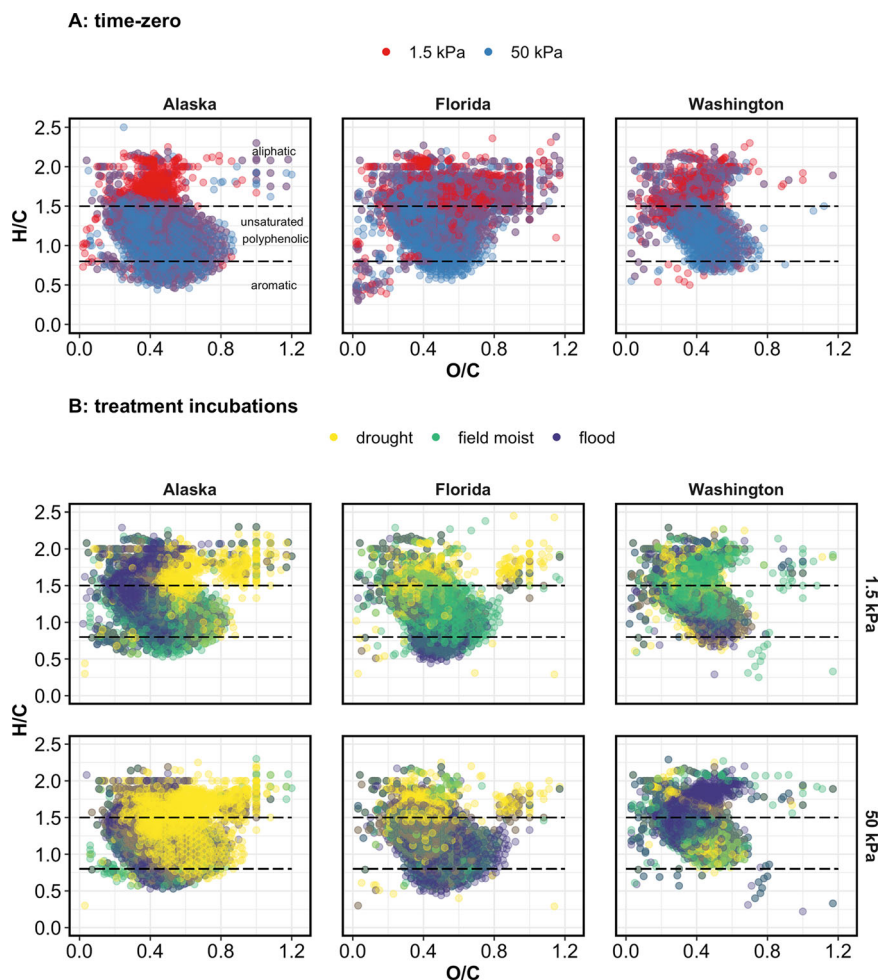


Fig. 2 Van Krevelen plots for Fourier transform ion cyclotron resonance mass spectrometry (FT-ICR-MS) resolved compounds, plotted using molecular H/C and O/C ratios. The H/C and O/C ratios are used for molecular classification of the FT-ICR-MS-resolved peaks. The figures show all identified molecular formulas, for **A** time-zero samples, i.e., native, unmanipulated soils (red = 1.5 kPa, blue = 50 kPa), and **B** for the incubated soils, in the coarse (>200 μm , 1.5 kPa) and fine (6–20 μm , 50 kPa) pore throats. Colors represent treatments (yellow = drought, green = field moist, and dark blue = flood). The horizontal dashed lines divide the Van Krevelen space into the broad compound classes (aliphatic, unsaturated polyphenolic, and aromatic). Related Van Krevelen plots can be found in Supplementary Figs. S3 and S4.

experience periodic water fluctuations between wet and dry, and being sandy, do not retain much water.

We identified differential expression of a number of sporulation and osmoprotectant synthesis genes in response to the moisture extremes of drought and flood. Notably, drought stimulated an increase in eight genes linked with sporulation (*spoVID*, *spoIIAB*, *spoIIID*, *spoIVA*, *spoIIAA*, *spoVT*, *spoOA*, and *spoVD*; Fig. 3A). Surprisingly, flood samples also showed increased expression of six genes involved in sporulation (*spoIIID*, *spoVT*, *spoIVA*, *spoOA*, *sigK*, and *sigE*; Fig. 3B), suggesting that sporulation may have been a response to both kinds of stress—too little as well as too much water. It is also possible that the physical disturbance of sampling caused stress to the microbial communities. Drought also stimulated osmoprotectant synthesis genes, such as *treC* and *betB* (Fig. 3A), which are involved in synthesis of trehalose and glycine betaine, respectively^{32,34}. These stress responses were seen in the Washington and Alaska soils. Florida soils showed no difference in gene expression due to drought or flood; however, it is important to note that these soils had fewer sequencing replicates due to low RNA recoveries from some samples.

Expression of several gliding motility genes was significantly decreased following drought, but only for the Alaska soils,

supporting hypothesis H2 for this site (Fig. 3A). However, these soils also showed increased expression of flagellar motility genes, suggesting that the microbes were likely producing more “swimming” apparatus to combat the low water conditions³⁵. Microbes are largely presumed to be fixed to soil minerals^{36,37}, although little research has been done to evaluate the relative contributions of fixed vs. planktonic microbes in soils. The presence of gliding motility genes is consistent with the availability of water-filled pore networks that would facilitate microbial distribution through the soil³⁸. The Washington soils had a high expression of gliding motility genes even in the drought treatment (Fig. 3A); these soils had a high residual water content (Table 1), and therefore it is likely that these soils may not have achieved an effective drought to elicit microbial response. The Florida soils had low expression of gliding motility at baseline conditions reflective of the low water content of these soils at baseline conditions.

Texture and disturbance history drive soil response to water fluctuations. Our goal was to evaluate possible common pathways of soil response to moisture fluctuations. We intentionally selected sites with different pedology and climatic conditions to

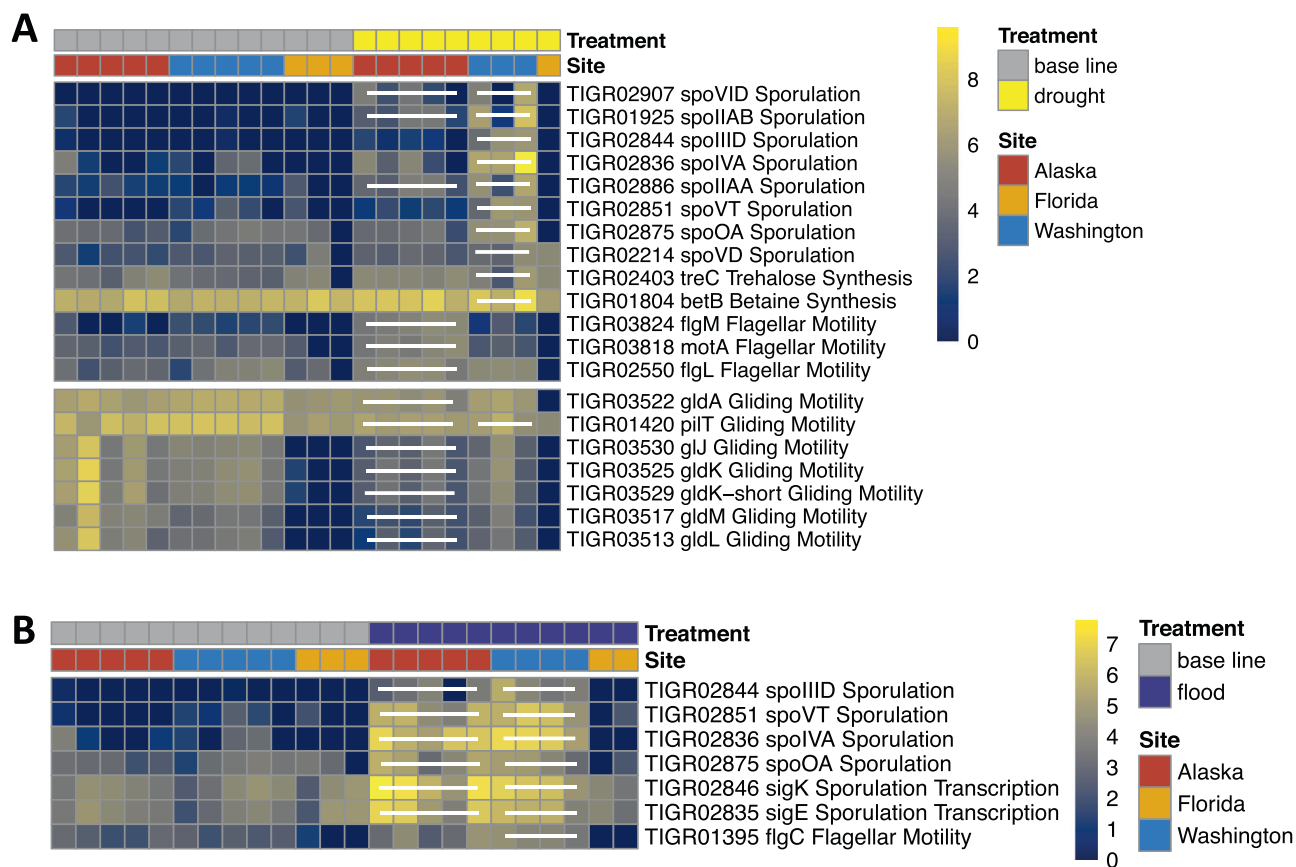


Fig. 3 Heatmap showing genes whose expression differed significantly among treatments. Differences are presented for **A** baseline vs. drought treatments, and **B** baseline vs. flood treatments. Gene families were identified using DESeq2. Heatmap colors indicate normalized abundances. Cells with white lines denote significant effect of drought or flood within a site ($\alpha = 0.05$).

see if, despite contrasting features, these soils would show consistent responses to drying and saturating conditions. However, this was not the case, and the complex results we present here must be considered within the context of the origin and structure of the soil at each site.

The Alaskan site has limited C inputs, a history of freezing stress, and silt-loam soils with limited C inputs. The history of freezing stress at this site can be considered as similar to drought history in some respects (e.g., lack of freely available water), but freezing does not have the same physicochemical effects as drought (e.g., changes in ionic strength and desorption of C), and the annual freeze–thaw regime is highly regular and predictable, unlike drought. These soils were ~15% clay (Supplementary Table S1), which likely played a role in SOC stabilization^{39,40}. As a result, these soils would have a high potential for SOM desorption/destabilization when experiencing drought conditions^{12,22}. While the drought increased the abundance of more saturated and oxidized molecules, the exact origin of these molecules is uncertain. It is possible that these molecules were previously held to mineral surfaces and then desorbed^{12,22,24}, or that these were formed by microbial metabolism of complex molecules⁴¹.

The microbial community in the Florida soil is likely adapted to moisture extremes, since the field site regularly cycles between wet and moist, but its soils also drain well due to the sandy texture. Since these microbes are presumably adapted to moisture fluctuations, it is likely that this adapted community will continue to metabolize and mineralize C, preferentially consuming simple aliphatic molecules. The Florida soils are sandy, and it is likely that microbes had greater access to simple molecules usually seen

more abundantly in macropores²¹. These simple molecules were consumed in the Florida soils, causing an enrichment of lignin-like and complex aromatic molecules across all treatments. The low clay content also suggests that the contribution of organo–mineral interactions to SOM stabilization would be quite low in these soils, and thus that the SOC would be more sensitive to physical disturbances during sampling.

The Washington State soils were sampled along a river floodplain, and the microbial communities are adapted to daily fluctuating saturated conditions. In fact, the field moisture content for these soils was very similar to the saturation water content (Table 1), explaining the lack of response to the flood treatment. In a wet system, such as the Washington cores sampled, flood would not be expected to stress the system. The minimal response of the soil chemistry to drought (Fig. 2) appears to be a consequence of the physical organization and pore structure of these soils. The size distribution of macropores (>50 μm) was approximately similar for the three soils (Supplementary Table S4), but the “dry” condition represented a residual water content of ~60% w/w for Washington, in stark contrast the Alaska and Florida soils (Table 1). The Washington soils also had greater pore and hydrologic connectivity (Supplementary Fig. S8), allowing for stronger buffering against moisture stress. Despite minimal effect on the pore-scale chemistry, the Washington drought soils exhibited the CO_2 flush usually seen upon rewetting dry soils due to physicochemical destabilization of protected C^{9,11–13}, microbial cell lysis⁴², and consequent changes in microbial activity⁴³ (Supplementary Figs. S9–S11). This suggests some transient response to drought, likely from the macropores, since (as noted) the micropores held ~60% moisture under these

“drought” conditions. There thus seems to be a disconnect between the core-scale gas flux response and the pore-scale molecular response for these soils, and may be a function of the high clay content and pore size distribution in these soils.

Conclusions and implications

Our first two hypotheses were partially supported, as (i) drought increased sporulation and osmoprotectant expression in the Alaska and Washington soils, and (ii) although flood did not significantly alter motility genes, drought did decrease the expression of gliding motility genes in the Alaska soils. Contrary to our predictions (hypothesis (i)), drought did not increase the abundance of complex aromatic compounds, but there was a distinct shift in the pore-water chemistry of the Alaska soils to more oxidized molecules.

Our experiment provides insight into potential controls on soil C processes, while demonstrating a long-recognized problem: it is difficult to unambiguously identify fully generalizable soil responses because of the complexity and heterogeneity of soils. This is true even for studies with very high numbers of samples or study sites. Nonetheless, our results provide insights on some potential pedologic and environmental controls on soil C processes. In particular, as we describe in Fig. 4, soil texture—and as a consequence, pore size distribution and spatial distribution of water—may drive the chemical response, whereas environmental conditions and disturbance history may drive the microbial response, of soils to new hydrologic regimes.

Related to the latter point is the concept of ecological stress⁴⁴, as changes in the microenvironment may not always be stressful for the system. We operationally define drought (air-drying to constant

weight) and flood (water imbibition to constant weight) in this experiment, and these terms may mean different things for different soils, and this may influence how each soil responds to the experimental treatment. For instance, even though all three soils were subjected to flood (i.e., 100% saturation), the amount of water imbibed differed by site. For Washington soils, with high field moisture content, the flooding treatment would not be expected to stress the system. Similarly, the Florida soils had a field moisture content of <10% w/w (Table 1 and Fig. 4), and would not respond strongly to a simulated drought. We are cautious not to overinterpret our results; the sample size is small, and we do not account for other variables, such as mineralogy, litter quality, etc. Nonetheless, this study allows us to propose an initial experimental framework to be built upon by future research and underlines the utility of incorporating environmental history and soil physicochemical properties, when studying biogeochemical processes to understand soil C–water dynamics at the pore-to-core scale.

Methods

Site description

Alaska. The CPRW at 65.162° N, 147.487° W is one of the primary research sites of the Bonanza Creek Long-Term Ecological Research Program in interior Alaska⁴⁵. The soil is Gilmore silt loam, poorly to well drained (loamy-skeletal, mixed, superactive, shallow Typic Dystrocrepts). Black spruce and feather mosses are the dominant vegetation. Upland mineral soils are adjacent to streams and wetlands vulnerable to hydrological modification from precipitation or permafrost changes.

Florida. The DWP site is near Kissimmee, FL, USA (28.105° N, 81.419° W)⁴⁶. DWP has a humid, subtropical climate with a mean annual temperature of 22.4 °C and precipitation of 1222 mm year⁻¹. Samples were collected from a pine flatwood stand at DWP. The soils are dominated by sandy textures and are classified as Immokalee Series (sandy, siliceous, hyperthermic Arenic Alaquods). The soils show moderate to high levels of organic matter (OM) accumulation at the surface.

Washington. The Secret River (SR) site at 46.308° N, 123.690° W consists of poorly drained floodplains along the SR, a tributary to Grays Bay in WA, USA⁴⁷. Tidal freshwater featuring an extensive network of tidally filled underground channels that fill and recede daily. Vegetation at the site is dominated by Sitka spruce and the soils are classified as Ocosta silty clay loam (fine, mixed, superactive, acid, isomesic Sulfic Endoaquepts).

Soil sampling and incubations. Intact soil cores (5 cm diameter, 15 cm height) were sampled (Alaska September 2016; Florida June 2016; and Washington October 2016), placed in a cooler on blue ice and shipped immediately to the Pacific Northwest National Laboratory in Richland, WA, USA, where they arrived within 36 h of sampling.

Each soil was subjected to one of three treatments, and each treatment was replicated on five cores:

- A set of cores was immediately saturated from below and incubated for 30 days (“flood”).
- A second set of cores was allowed to air-dry until constant weight was reached for five consecutive days, after which they were incubated at dry conditions for 30 days (“drought”).
- A third set of cores was maintained at the field-moist water content, for 30 days (“field moist”). The field-moist treatment was used to determine soil C processes under partially saturated conditions occurring in the field, reflecting discontinuous resource islands in the soil cores.

At the end of the 30-day incubations, the cores were saturated from below and held at saturated conditions for 24 h. This was done to capture the CO₂ fluxes that typically occur during rewetting^{8–10}, and also to prepare the cores for pore-water extraction (see below). We had two additional sets of cores as controls—“baseline” samples that were immediately deconstructed, and a “time-zero saturation” group of cores that were saturated and immediately deconstructed for analysis. All incubations were conducted at 21 °C, in the dark, under ambient relative humidity (18%). We had five replicates ($n = 5$) per site-treatment combination.

We monitored CO₂ and methane (CH₄) production every 3 days during the 30-day incubations, and hourly during the post-incubation saturation. The gas concentrations were measured in the cores’ headspace, using a G2301 Picarro GHG analyzer (Picarro, Sunnyvale, CA, USA). Fluxes were computed from the concentration changes according to the equation

$$A = (dC/dt * V/M * Pa/RT)$$

where A is the flux ($\mu\text{mol g soil}^{-1} \text{s}^{-1}$), dC/dt the rate of change in gas concentration (mole fraction s^{-1}), V the total chamber volume (cm^3), M dry soil

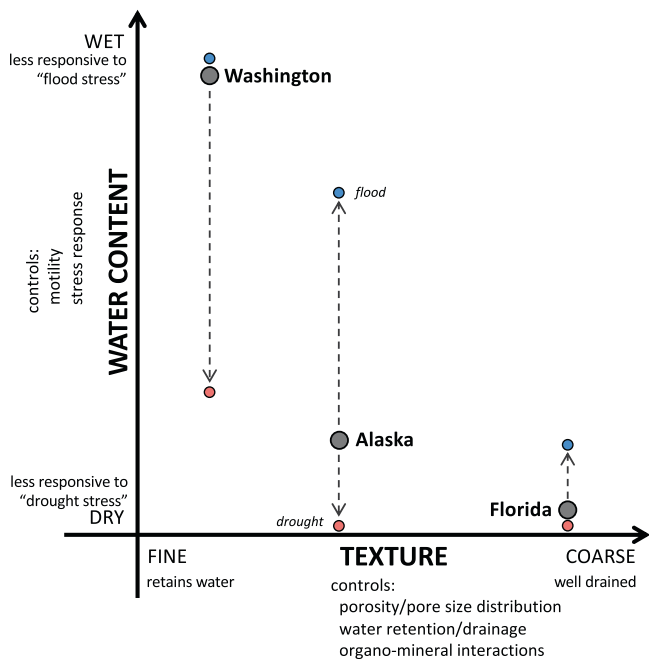


Fig. 4 The three soils in this experiment, represented as a function of water content and texture. We show the range of soil moisture experienced by these soils during the experimental incubations—the larger, gray circles represent field-moist water content, and the smaller circles represent moisture content for drought (red)/flood (blue) treatments. Soil texture appears to drive the chemical response by controlling porosity and water retention, and field water content drives biological stress response to moisture fluctuations. The Washington soils had a high field moisture content, and therefore showed minimal response to the “flooding” treatment. On the other hand, the Florida soils had low field moisture content, and therefore showed minimal response to the “drought” treatment.

mass (g), P atmospheric pressure (kPa), R the universal gas constant ($8.3 \times 10^3 \text{ cm}^3 \text{ kPa mol}^{-1} \text{ K}^{-1}$), and T air temperature (K).

Pore-water extraction, core deconstruction, and analysis. At the end of the incubation, pore water was sampled following the procedure of Bailey et al.²¹. Cores were transferred onto individual 100 kPa Tempe Pressure Cell units fit with a high flow ceramic plate (Soil Moisture Equipment Corp. Goleta, CA, USA) to sequentially collect pore waters with suctions of -1.5 and -50 kPa, using a pump with a PCD Dual-Valve pressure controller (Alicat Scientific, Tucson, AZ). These suction values were used because they correspond to pore size diameters of $\sim 200 \mu\text{m}$ (coarse) and $6 \mu\text{m}$ (fine), respectively, using the Kelvin equation⁴⁸. Pore water was collected into borosilicate vials for 24 h, or until flow ceased at each suction setting and stored at -20°C until analysis. Pore-water samples were filtered through a $0.22 \mu\text{m}$ Sterivex filter immediately prior to being analyzed. Pore-water samples were analyzed for total DOC via combustion catalytic oxidation (TOC-5000A TOC Analyzer, Shimadzu). The molecular composition of the dissolved C was characterized by electrospray ionization coupled with FT-ICR-MS. The samples were desalted by solid-phase extraction with PPL cartridges⁴⁹. Detailed description of the analysis and data handling are provided below.

Cores were deconstructed following pore-water removal and the soils were sieved through 4 mm mesh to remove roots and rocks. The sieved soil was subsampled for the measurements outlined below.

Water soluble organic carbon (WSOC) was extracted from air-dried soil (1:5 soil volume: Milli-Q water) by shaking at 4°C on a reciprocal shaker set at 200 r.p.m. high at 200 r.p.m. for 2 h, centrifuging for 5 min at 10,000 r.c.f., and then filtering through $0.22 \mu\text{m}$ Sterivex™ filters. An aliquot (1.5 mL) was stored at -20°C for downstream analyses of FT-ICR-MS—used to measure changes in soil soluble carbon chemistry. The remaining sample was stored at -20°C until measured for total dissolved carbon on a Shimadzu TOC-5000A. Soils were air-dried for total C and total organic C (TOC) and were analyzed on a VarioEL Cube Elemental Analyzer (Elementar Analysensysteme GmbH, Langensfeld, Germany).

DNA and RNA were extracted from soil using the Qiagen PowerSoil DNA and Qiagen PowerSoil RNA extraction kit respectively, according to the manufacturer's instructions. DNA concentrations were determined using a Qubit 2.0 Fluorometer using the dsDNA HS (ThermoFisher Scientific). Shotgun metagenome sequencing on an Illumina HiSeq 1500 was used to estimate microbial potential.

RNA extracts were further purified with a PowerClean® RNA Clean-Up Kit (MO BIO, Carlsbad, CA) and analyzed for concentration, ribosomal RNA (rRNA) ratio, and RNA integrity number (RIN) on a 2100 Bioanalyzer (Agilent Technologies, Santa Clara, CA), using the RNA 6000 Nano kit (Agilent Technologies, Santa Clara, CA). Only samples with a RIN (RNA integrity) value of 8 and above were prepared for sequencing. rRNA was depleted prior to sequencing using the Ribo-Zero magnetic gold kit (Epidemiology). Bacterial mRNA thus obtained was purified using AMPure RNAClean XP beads. cDNA synthesis and library preparation were carried out using random hexamers and the ScriptSeq v2 RNA-Seq Kit (Epicenter). Metatranscriptome libraries were sequenced on the HiSeq 2500 platform (Illumina, San Diego, CA) on a paired-end flow-cell at 2×250 cycles.

FT-ICR-MS analysis. FT-ICR-MS analysis was performed on a 21 T FT-ICR mass spectrometer at the Environmental Molecular Sciences Laboratory (EMSL) in Richland, WA⁵⁰. Ninety-six individual scans were averaged for each sample and internally calibrated using OM homologous series separated by 14 Da ($-\text{CH}_2$ groups). The mass measurement accuracy was <1 p.p.m. for singly charged ions across a broad m/z range ($200 < m/z < 1200$). Chemical formulas were assigned using in-house software based on the Compound Identification Algorithm described by Kujawinski & Behn⁵¹ and modified by Minor et al.⁵². Chemical formulas were assigned based on the following criteria: signal-to-noise (S/N) > 7 , and mass measurement error < 1 p.p.m., taking into consideration the presence of C, H, O, N, S, and P and excluding other elements.

Further processing of these data was done using the *fticrr* workflow in R⁵³. FT-ICR-MS spectra were classified into eight biomolecular groups, referred to as FT-ICR compound classes, using the Van Krevelen classification based on molecular O/C and H/C ratios^{26,27}; lipids ($0 < \text{O/C} \leq 0.3$, $1.5 \leq \text{H/C} \leq 2.5$), unsaturated hydrocarbons ($0 \leq \text{O/C} \leq 0.125$, $0.8 \leq \text{H/C} < 2.5$), proteins ($0.3 < \text{O/C} \leq 0.55$, $1.5 \leq \text{H/C} \leq 2.3$), amino sugars ($0.55 < \text{O/C} \leq 0.7$, $1.5 \leq \text{H/C} \leq 2.2$), carbohydrates ($0.7 < \text{O/C} \leq 1.5$, $1.5 \leq \text{H/C} \leq 2.5$), lignin ($0.125 < \text{O/C} \leq 0.65$, $0.8 \leq \text{H/C} < 1.5$), tannins ($0.65 < \text{O/C} \leq 1.1$, $0.8 \leq \text{H/C} < 1.5$), and condensed hydrocarbons ($0 \leq \text{O/C} \leq 0.95$, $0.2 \leq \text{H/C} < 0.8$). The distribution of compound classes is shown in Supplementary Fig. S1a. FT-ICR compound classes are tentative classifications as they are solely based on the O/C and H/C ratios from the molecular formula, not the molecular structure. As such, it would be more accurate to describe compounds as lipid-like or carbohydrate-like. For simplicity, we refer to each compound class, however, as lipids, tannins, proteins, and so on. Relative abundance values were calculated from count values associated with each observed biomolecule group normalized by the total number of C molecules identified.

FT-ICR-MS data were analyzed using multivariate analysis of variance (MANOVA). Treatment effect on WSOC composition was determined using group-wise relative abundance as the response variable. Due to the significant

interaction of treatment and pore size class, the 1.5 and 50 kPa pore size classes were analyzed separately. Principal components analysis (PCA) was performed using the *stats* package in R, and was visualized using the *ggbiplot* package⁵⁴.

Metagenome and metatranscriptome data processing. Metagenomic and metatranscriptomic reads were cleaned using *bbduk*, and paired-end reads were merged using *bbmerge*. Reads were then annotated to TIGRFAMS gene families using *MaxRebo* (McCue, unpubl.). For DNA and RNA analyses, we first removed all ribosomal genes before normalizing by relative abundance. We then removed any genes that had $<0.001\%$ relative abundance in all samples.

Due to the nonparametric nature of metagenome and metatranscriptome data, PCAs for these data were generated with Euclidean distances using *vegan* v2.5-5 (ref. 55), and significance testing was performed using the *adonis* function in *vegan*. To identify discriminatory genes across the three sites, we used linear discriminant analysis effect size (LEfSe⁵⁶) to identify the top 20 genes that were significantly enriched in each location and/or treatment, and had a logarithmic score > 2 . For gene expression analysis comparing drought and flood to baseline, we used the *DESeq2* package⁵⁷ to identify significant transcripts and calculate \log_2 fold change. For heatmap coloring, we normalized gene abundances using the *normTransform()* function from the *DESeq2* package, and colored the resulting values using the *cividis* color palette⁵⁸.

Additional soil characterization. The time-zero soils were also analyzed for pH, electrical conductivity, basic nutrients (P, K, Ca, Mg, etc.), and particle size distribution at the Oregon State University Central Analytical Laboratory (Supplementary Table S1).

Pore size distribution was determined using X-ray computed tomography on an X-Tek/Metris XTH 320/225 kV scanner (Nikon Metrology, Belmont, CA). Data were collected at 110 kV and 265 μA X-ray power. The core samples were rotated continuously during the scans with momentary stops to collect each projection (shuttling mode), while minimizing ring artifacts. A total of 3142 projections were collected over 360° with 0.5 s exposure time and four frames per projection. Image voxel size was $28 \mu\text{m}$. The images were reconstructed to obtain 3D data sets using CT Pro 3D (Metris XT 2.2, Nikon Metrology). Representative slice and 3D images were created using VG Studio MAX 2.1 (Volume Graphics GmbH, Heidelberg Germany). Image processing and porosity analysis (including pore volume segmentation and pore analysis) was carried out using ImageJ 1.51k (National Institute of Health, USA).

The water retention characteristic (desorption/drying curve) was determined by saturating soil samples and subsequently drying by evaporation at room temperature. Changes in weight and water tension were measured using a HYPROP® (METER Environment Inc., USA) every 10 min for 7 days. The data were fit using the van Genuchten equation⁵⁹ to generate relationships of water tension vs. water content for the three soils.

All data analyses were performed in R version 3.6.0 (2019-04-26)⁶⁰, using mainly *dplyr* v1.0.4⁶¹ for data processing and *ggplot2* v3.3.3⁶² for data visualization.

Data availability

The data and R scripts are available online at https://github.com/kaizadp/TES_3Soils_2021 (<https://doi.org/10.5281/zenodo.4792655>) and are archived at the Department of Energy's Environmental Systems Science Data Infrastructure for a Virtual Ecosystem (ESS-DIVE) data repository (<https://doi.org/10.15485/1785525>).

Received: 7 August 2020; Accepted: 6 May 2021;

Published online: 15 June 2021

References

- Vousdoukas, M. I. et al. Global probabilistic projections of extreme sea levels show intensification of coastal flood hazard. *Nat. Commun.* **9**, 2360 (2018).
- Rahmstorf, S. Rising hazard of storm-surge flooding. *Proc. Natl. Acad. Sci. USA* **114**, 11806–11808 (2017).
- Manzoni, S., Ahmed, M. H. & Porporato, A. Ecohydrological and stoichiometric controls on soil carbon and nitrogen dynamics in drylands. In *Dryland Ecohydrology* (eds D'Odorico, P., Porporato, A. & Wilkinson, C.) 279–307 (Springer International Publishing, 2019).
- Liu, Y. et al. Modeling transient soil moisture limitations on microbial carbon respiration. *J. Geophys. Res. Biogeosci.* **124**, 2222–2247 (2019).
- Hawkes, C. V., Waring, B. G., Rocca, J. D. & Kivlin, S. N. Historical climate controls soil respiration responses to current soil moisture. *Proc. Natl. Acad. Sci. USA* **114**, 6322–6327 (2017).
- Manzoni, S. et al. Rainfall intensification increases the contribution of rewetting pulses to soil respiration. *Biogeosci.* **17**, 4007–4023 (2020).
- Patel, K. F. et al. Soil carbon dynamics during drying vs. rewetting: Importance of antecedent moisture conditions. *Soil Biol. Biochem.* **156**, 108165 (2021).
- Borken, W. & Matzner, E. Introduction: Impact of extreme meteorological events on soils and plants. *Glob. Chang. Biol.* **15**, 781 (2009).

9. Slessarev, E. W. & Schimel, J. P. Partitioning sources of CO₂ emission after soil wetting using high-resolution observations and minimal models. *Soil Biol. Biochem.* **143**, 107753 (2020).
10. Kim, D.-G., Vargas, R., Bond-Lamberty, B. & Turetsky, M. R. Effects of soil rewetting and thawing on soil gas fluxes: a review of current literature and suggestions for future research. *Biogeosciences* **9**, 2459–2483 (2012).
11. Jarvis, P. et al. Drying and wetting of Mediterranean soils stimulates decomposition and carbon dioxide emission: the “Birch effect”. *Tree Physiol* **27**, 929–940 (2007).
12. Bailey, V. L., Pries, C. H. & Lajtha, K. What do we know about soil carbon destabilization? *Environ. Res. Lett.* **14**, 083004 (2019).
13. Moyano, F. E. et al. The moisture response of soil heterotrophic respiration: interaction with soil properties. *Biogeosciences* **9**, 1173–1182 (2012).
14. Huntington, T. G. Evidence for intensification of the global water cycle: review and synthesis. *J. Hydrol.* **319**, 83–95 (2006).
15. Durack, P. J., Wijffels, S. E. & Matear, R. J. Ocean salinities reveal strong global water cycle intensification during 1950 to 2000. *Science* **336**, 455–458 (2012).
16. Chowdhury, N., Marschner, P. & Burns, R. Response of microbial activity and community structure to decreasing soil osmotic and matric potential. *Plant Soil* **344**, 241–254 (2011).
17. Dyer, C. L., Kopittke, P. M., Sheldon, A. R. & Menzies, N. W. Influence of soil moisture content on soil solution composition. *Soil Sci. Soc. Am. J.* **72**, 355–361 (2008).
18. Negassa, W. C. et al. Properties of soil pore space regulate pathways of plant residue decomposition and community structure of associated bacteria. *PLoS ONE* **10**, 1–22 (2015).
19. Yan, Z. et al. Pore-scale investigation on the response of heterotrophic respiration to moisture conditions in heterogeneous soils. *Biogeochemistry* **131**, 121–134 (2016).
20. van Genuchten, M. T. & Pachepsky, Y. A. Hydraulic properties in unsaturated soils. In *Encyclopedia of Agrophysics* (eds Gliński, J., Horabik, J. & Lipiec, J.) 368–376 (Springer, 2011).
21. Bailey, V. L., Smith, A. P., Tfaily, M., Fansler, S. J. & Bond-Lamberty, B. Differences in soluble organic carbon chemistry in pore waters sampled from different pore size domains. *Soil Biol. Biochem.* **107**, 133–143 (2017).
22. Newcomb, C. J., Qafoku, N. P., Grate, J. W., Bailey, V. L. & De Yoreo, J. J. Developing a molecular picture of soil organic matter–mineral interactions by quantifying organo-mineral binding. *Nat. Commun.* **8**, 1–8 (2017).
23. Meier, C. L. & Bowman, W. D. Links between plant litter chemistry, species diversity, and below-ground ecosystem function. *Proc. Natl. Acad. Sci. USA* **105**, 19780–19785 (2008).
24. Kaiser, M., Kleber, M. & Berhe, A. A. How air-drying and rewetting modify soil organic matter characteristics: an assessment to improve data interpretation and inference. *Soil Biol. Biochem.* **80**, 324–340 (2015).
25. Blazewicz, S. J., Schwartz, E. & Firestone, M. K. Growth and death of bacteria and fungi underlie rainfall-induced carbon dioxide pulses from seasonally dried soil. *Ecology* **95**, 1162–1172 (2014).
26. Tfaily, M. M. et al. Advanced solvent based methods for molecular characterization of soil organic matter by high-resolution mass spectrometry. *Anal. Chem.* **87**, 5206–5215 (2015).
27. Sleighter, R. L. & Hatcher, P. G. The application of electrospray ionization coupled to ultrahigh resolution mass spectrometry for the molecular characterization of natural organic matter. *J. Mass Spectrom.* **42**, 559–574 (2007).
28. Graham, E. B., Tfaily, M. M. & Crump, A. R. Carbon inputs from riparian vegetation limit oxidation of physically bound organic carbon via biochemical and thermodynamic processes. *J. Geophys. Res. Biogeosci.* **122**, 3188–3205 (2017).
29. LaRowe, D. E. & Van Cappellen, P. Degradation of natural organic matter: a thermodynamic analysis. *Geochim. Cosmochim. Acta* **75**, 2030–2042 (2011).
30. Jansson, J. K. & Hofmockel, K. S. The soil microbiome—from metagenomics to metaphenomics. *Curr. Opin. Microbiol.* **43**, 162–168 (2018).
31. Roy Chowdhury, T. et al. Metaphenomic responses of a native prairie soil microbiome to moisture perturbations. *mSystems* **4**, e00061–19 (2019).
32. Warren, C. R. Do microbial osmolytes or extracellular depolymerisation products accumulate as soil dries? *Soil Biol. Biochem.* **98**, 54–63 (2016).
33. Schimel, J. P. Life in dry soils: effects of drought on soil microbial communities and processes. *Annu. Rev. Ecol. Evol. Syst.* **49**, 409–432 (2018).
34. Reina-Bueno, M. et al. Role of trehalose in heat and desiccation tolerance in the soil bacterium *Rhizobium etli*. *BMC Microbiol.* **12**, 207 (2012).
35. Blair, D. F. How bacteria sense and swim. *Annu. Rev. Microbiol.* **49**, 489–522 (1995).
36. Holm, P. E., Nielsen, P. H., Albrechtsen, H. J. & Christensen, T. H. Importance of unattached bacteria and bacteria attached to sediment in determining potentials for degradation of xenobiotic organic contaminants in an aerobic aquifer. *Appl. Environ. Microbiol.* **58**, 3020–3026 (1992).
37. Kuz'yakov, Y. & Blagodatskaya, E. Microbial hotspots and hot moments in soil: concept & review. *Soil Biol. Biochem.* **83**, 184–199 (2015).
38. Tecon, R. & Or, D. Bacterial flagellar motility on hydrated rough surfaces controlled by aqueous film thickness and connectedness. *Sci. Rep.* **6**, 19409 (2016).
39. Lavelle, J. M., Soong, J. L. & Cotrufo, M. F. Conceptualizing soil organic matter into particulate and mineral-associated forms to address global change in the 21st century. *Glob. Chang. Biol.* **26**, 261–273 (2020).
40. Jilling, A. et al. Minerals in the rhizosphere: overlooked mediators of soil nitrogen availability to plants and microbes. *Biogeochemistry* **139**, 103–122 (2018).
41. Sinsabaugh, R. L. Phenol oxidase, peroxidase and organic matter dynamics of soil. *Soil Biol. Biochem.* **42**, 391–404 (2010).
42. Fierer, N. & Schimel, J. P. A proposed mechanism for the pulse in carbon dioxide production commonly observed following the rapid rewetting of a dry soil. *Soil Sci. Soc. Am. J.* **67**, 798 (2003).
43. Xiang, S.-R., Doyle, A., Holden, P. A. & Schimel, J. P. Drying and rewetting effects on C and N mineralization and microbial activity in surface and subsurface California grassland soils. *Soil Biol. Biochem.* **40**, 2281–2289 (2008).
44. Schimel, J. P., Balsler, T. C. & Wallenstein, M. D. Microbial stress-response physiology and its implications for ecosystem function. *Ecology* **88**, 1386–1394 (2007).
45. Petrone, K. C., Jones, J. B., Hinzman, L. D. & Boone, R. D. Seasonal export of carbon, nitrogen, and major solutes from Alaskan catchments with discontinuous permafrost. *J. Geophys. Res. Biogeosci.* **111**, 1–13 (2006).
46. McClellan, M., Comas, X., Benscoter, B., Hinkle, R. & Sumner, D. Estimating belowground carbon stocks in isolated wetlands of the northern Everglades watershed, Central Florida, using ground penetrating radar and aerial imagery. *J. Geophys. Res. Biogeosci.* **122**, 2804–2816 (2017).
47. Roy Chowdhury, T. et al. Temporal dynamics of CO₂ and CH₄ loss potentials in response to rapid hydrological shifts in tidal freshwater wetland soils. *Ecol. Eng.* **114**, 104–114 (2018).
48. Carson, J. K. et al. Low pore connectivity increases bacterial diversity in soil. *Appl. Environ. Microbiol.* **76**, 3936–3942 (2010).
49. Dittmar, T., Koch, B., Hertkorn, N. & Kattner, G. A simple and efficient method for the solid-phase extraction of dissolved organic matter (SPE-DOM) from seawater. *Limnol. Oceanogr. Methods* **6**, 230–235 (2008).
50. Shaw, J. B. et al. 21 Tesla fourier transform ion cyclotron resonance mass spectrometer greatly expands mass spectrometry toolbox. *J. Am. Soc. Mass Spectrom.* **27**, 1929–1936 (2016).
51. Kujawinski, E. B. & Behn, M. D. Automated analysis of electrospray ionization fourier transform ion cyclotron resonance mass spectra of natural organic matter. *Anal. Chem.* **78**, 4363–4373 (2006).
52. Minor, E. C., Steinbring, C. J., Longnecker, K. & Kujawinski, E. B. Characterization of dissolved organic matter in Lake Superior and its watershed using ultrahigh resolution mass spectrometry. *Organic Geochemistry* **43**, 1–11 (2012).
53. Patel, K. F. fticrr: FTICR-results-in-R <https://doi.org/10.5281/ZENODO.3893245> (2020).
54. Vu, V. Q. ggbiplot: A ggplot2 based biplot. R package version 0.55. <http://github.com/vqv/ggbiplot> (2011).
55. Oksanen, J. et al. vegan: Community Ecology Package. R package version 2.5–5. <https://CRAN.R-project.org/package=vegan> (2019).
56. Segata, N. et al. Metagenomic biomarker discovery and explanation. *Genome Biol.* **12**, R60 (2011).
57. Love, M. I., Huber, W. & Anders, S. Moderated estimation of fold change and dispersion for RNA-seq data with DESeq2. *Genome Biol.* **15**, 550 (2014).
58. Nuñez, J. R., Anderton, C. R. & Renslow, R. S. Optimizing colormaps with consideration for color vision deficiency to enable accurate interpretation of scientific data. *PLoS ONE* **13**, e0199239 (2018).
59. van Genuchten, M. T. A closed-form equation for predicting the hydraulic conductivity of unsaturated soils. *Soil Sci. Soc. Am. J.* **44**, 892–898 (1980).
60. R Core Team. R: A language and environment for statistical computing. <https://www.R-project.org/> (2020).
61. Wickham, H., François, R. & Lionel H. dplyr: A grammar of data manipulation. <https://CRAN.R-project.org/package=dplyr> (2020).
62. Wickham, H. *ggplot2: Elegant Graphics for Data Analysis* (Springer, 2016).

Acknowledgements

We are grateful to Amy Borde, Brian Benscoter, Carolyn Anderson, and Emily Graham for their help with field work and sampling. We also thank Malak Tfaily and Robert Danczak for providing guidance on FT-ICR-MS design and analysis. This research was supported by the U.S. Department of Energy, Office of Science, Biological and Environmental Research as part of the Environmental System Science Program. The Pacific Northwest National Laboratory is operated for DOE by Battelle Memorial Institute under contract DE-AC05-76RL01830. A portion of this research was performed using EMSL, a DOE Office of Science user facility sponsored by the Department of Energy's Office of Biological and Environmental Research and located at Pacific Northwest National Laboratory.

Author contributions

V.L.B. designed the experiment with help from B.B.-L., A.P.S., and T.R.C. A.P.S., T.R.C., B.B.-L., and S.J.F. collected samples and performed laboratory experiments. L.A.M. performed metagenome and metatranscriptome analyses, and T.V. performed tomography analysis. K.F.P. and T.P.C. performed data analysis, and K.F.P. wrote the manuscript with inputs from all the authors.

Competing interests

The authors declare no competing interests.

Additional information

Supplementary information The online version contains supplementary material available at <https://doi.org/10.1038/s43247-021-00198-4>.

Correspondence and requests for materials should be addressed to V.L.B.

Peer review information *Communications Earth & Environment* thanks the anonymous reviewers for their contribution to the peer review of this work. Primary handling editors: Joshua Dean, Joseph Aslin, Clare Davis. Peer reviewer reports are available.

Reprints and permission information is available at <http://www.nature.com/reprints>

Publisher's note Springer Nature remains neutral with regard to jurisdictional claims in published maps and institutional affiliations.



Open Access This article is licensed under a Creative Commons Attribution 4.0 International License, which permits use, sharing, adaptation, distribution and reproduction in any medium or format, as long as you give appropriate credit to the original author(s) and the source, provide a link to the Creative Commons license, and indicate if changes were made. The images or other third party material in this article are included in the article's Creative Commons license, unless indicated otherwise in a credit line to the material. If material is not included in the article's Creative Commons license and your intended use is not permitted by statutory regulation or exceeds the permitted use, you will need to obtain permission directly from the copyright holder. To view a copy of this license, visit <http://creativecommons.org/licenses/by/4.0/>.

© The Author(s) 2021